Molecular Crystals and Liquid Crystals Science and Technology. Section A. Molecular Crystals and Liquid Crystals

Publication details, including instructions for authors and subscription information:
http://www.tandfonline.com/loi/gmcl19

Selectively Deuterated Liquid Crystalline Cyanoazobenzene Side-Chain Polyesters. 1. Preparation and Characterization of Precursors and Diols

Claudia Hendann [a] , Heinz W. Siesler [a] , Fulvio Andruzzi [b] , Christian Kulinna [c] & Søren Hvilsted [c]

[a] Department of Physical Chemistry, University of Essen, D-45117, Essen, Germany

[b] Centro Studi Processi Ionici di Polimerizzazione, CNR, Dipartimento di Ingegneria Chimica, Facoltà di Ingegneria, Via Diotisalvi 2, I-56100, Pisa, Italy

[c] Department of Solid State Physics, Risø National Laboratory, DK- 4000, Roskilde, Denmark

Version of record first published: 04 Oct 2006

To cite this article: Claudia Hendann, Heinz W. Siesler, Fulvio Andruzzi, Christian Kulinna & Søren Hvilsted (1998): Selectively Deuterated Liquid Crystalline Cyanoazobenzene Side-Chain Polyesters. 1. Preparation and Characterization of Precursors and Diols, Molecular Crystals and Liquid Crystals Science and Technology. Section A. Molecular Crystals and Liquid Crystals, 319:1, 207-230

To link to this article: http://dx.doi.org/10.1080/10587259808045660

Mol. Cryst. Liq. Cryst., Vol. 319, pp. 207–230
Reprints available directly from the publisher
Photocopying permitted by license only

Selectively Deuterated Liquid Crystalline Cyanoazobenzene Side-Chain Polyesters. 1. Preparation and Characterization of Precursors and Diols

CLAUDIA HENDANN[a], HEINZ W. SIESLER[a], FULVIO ANDRUZZI[b], CHRISTIAN KULINNA[c] and SØREN HVILSTED[c,*]

[a] *Department of Physical Chemistry, University of Essen, D-45117 Essen, Germany;*
[b] *Centro Studi Processi Ionici di Polimerizzazione, CNR, Dipartimento di Ingegneria Chimica, Facoltà di Ingegneria, Via Diotisalvi 2, I-56100 Pisa, Italy;*
[c] *Department of Solid State Physics, Risø National Laboratory, DK-4000 Roskilde, Denmark*

(Received in final form 18 July 1996)

Diphenyl perdeuterated adipate and tetradecanedioate, and three different, selectively deuterium labeled 2-[6-[4-[(4-cyanophenyl)azo]phenoxy]hexyl]-1,3-propanediols have been prepared by exchange and reduction techniques. ^{1}H and ^{2}H NMR spectroscopic investigations have revealed the deuterium exchange in the esters to be higher than 93% and evenly distributed. Similarly, a varying but high deuterium exchange was detected in the selectively labeled diols. All deuterated samples were additionally characterized in detail by ^{13}C NMR spectroscopy; the deuterium isotope effect conclusively assisted some of the shift assignments. No isotope effect could be detected by visible spectroscopy in any of the deuterated diols. On the other hand, FTIR in all deuterated compounds reveals a substantial frequency shift of all carbon–deuteron vibrations as compared to the corresponding carbon–hydrogen vibrations. Polarizing optical microscopic and differential scanning calorimetric investigations have identified all the deuterium labeled diols as monotropic liquid crystals with both nematic and smectic A phases.

Keywords: Deuterated liquid crystals; cyanoazobenzene liquid crystals; side-chain polyesters; diols; spectroscopy of liquid crystals

* Corresponding author. Tel: +45 46 77 47 84; Fax: +45 46 77 47 91;
e-mail: s.hvilsted@risoe.dk

1. INTRODUCTION

The search for polymeric materials capable of reversible optical information storage has increased through the last decade [1, 2]. In particular, the photochromic properties of azobenzene [3] has attracted tremendous attention. Different systems with azo dyes dispersed in polymers [4, 5], azobenzene side-chains in unoriented amorphous [6, 7], or prealigned liquid crystalline polymers [8–12] have been proposed and investigated. Our recently introduced system based on liquid crystalline cyanoazobenzene side-chain polyesters [13] have some intriguing and challenging properties. Thus, unoriented thin films of these polyesters possess very high diffraction efficiency of approx. 40% obtained by polarization recording of high density gratings (more than 5000 lines/mm) with no sign of decay for almost four years [14]. However, the stored information can be erased by heating the films to about 80°C and after cooling to room temperature the film can be reused [15]. The stored information can also be erased using light [16]. In this case the anisotropy was induced in the film at 488 nm from an Argon laser for a period of 500 ms, read-out at 633 nm for a period of 300 ms and erased by light at 351 nm from a Krypton laser for 200 ms. These cycles have been repeated 10,000 times. The resulting anisotropy in these polyester materials photoinduced by *trans-cis-trans* azobenzene cycles has been studied in detail by focusing on the dichroic behaviour of the nitrile vibrational band employing polarized FTIR spectroscopy [17]. Recently, it was also shown for the first time experimentally by use of optical and IR spectroscopy that a red laser beam at 633 nm causes *cis-trans* transitions in azobenzene side-chain polyesters [18].

So far only the terminal cyano substituent extending the long axis of the azobenzene chromophore in the *trans* ground state has been accessible to the dichroic, spectroscopic FTIR analysis. It has long been speculated [19] that not only the photo addressable azobenzene chromophore furnish the anisotropy but also other material segments could contribute the final material anisotropy. Additional indications have been provided by atomic force and scanning near-field optical microscopic investigations [20]. However, the chemical similarity of the other main constituents of the polyester system, the methylene flexible spacer and main-chain segment, makes them inaccessible to a dichroic FTIR analysis. Consequently, a methodology enabling the study of fundamental segmental mobility was aimed at. The most pertinent and powerful molecular marking tool seems to be strategic proton exchange with deuteron. Chemically several exchange

possibilities are available and spectroscopically large impact is to be expected [21, 22].

This paper outlines the synthetic approach necessary to produce selectively deuterated precursors and diols suitable for the previously developed polyester preparative strategy. Furthermore, a comprehensive thermal and spectroscopic analysis of all deuterated compounds especially focusing on multinuclei NMR and FTIR spectroscopy will be presented.

2. EXPERIMENTAL SECTION

2.1. Synthesis

The starting materials were generally of the purest kind available and used as received. The inorganic chemicals were all analytical grade. All solvents were analytical grade and used as received unless otherwise specified.

Perdeutero-tetradecanedioic Acid (1)

Perdeutero-tetradecanedioic acid was prepared by a high temperature, catalytic exchange reaction employing D_2O as deuterium source and Pt/C as heterogeneous catalyst [23]. Tetradecanedioic acid was kept in form of the sodium salt for 9 days at 195°C in a sealed glass tube inside a rotating stainless steel reactor containing some D_2O for pressure equilibration. After hot filtration from the catalyst, the solution was acidified and the precipitated acid vacuum dried (yield 74%). The perdeuterated acid was used without further purification. The deuterium content of the tetradecanedioic acid after one exchange step is approximately 90–93% as determined by high resolution ^{1}H NMR spectroscopy using phenol as internal standard. Since deuterium incorporation of 70–80% was found to be sufficient for infrared and ^{2}H NMR studies [24], only one exchange procedure was employed to avoid material losses.

Diphenyl Esters (2–5)

Perdeutero-adipic acid, commercially obtained from IC-Chemikalien GmbH Germany, has an isotope content of 99% (confirmed by ^{1}H NMR). The perdeuterated and non-deuterated acids were converted to the corresponding dichlorides by refluxing with thionyl chloride. After removal of excess thionyl chloride the dichlorides were converted directly to the

diphenyl esters by a pyridine catalyzed acylation as described previously [25]. Recrystallisation twice from methanol was found sufficient to yield the required purity of the diphenyl esters for the polycondensation reaction. Melting points of the perdeuterated esters were determined by DSC at a heating rate of 3°C/min to 80.9°C (tetradecanedioate, **2**) and 109.3°C (adipate, **4**), respectively.

2-[6-[4-[(4-cyanophenyl)azo] phenoxy]-1,1,2,2,5,5,6,6-octadeuterohexyl]-1,3-propanediol (9)

Deuteration in the α-positions of adipic acid was achieved by dissolving the sodium salt in D_2O and heating the solution to 150°C for 24 hours [26]. The resulting solvent was then removed by Rotary evaporation, replaced with new D_2O and the procedure repeated. Following acidification 2,2,5,5-tetradeuteroadipic acid was recovered by continuous extraction with diethyl ether after a total of five repetitive exchange procedures. A deuterium content of 80% in the α-positions was determined by ^{1}H NMR. Conversion of this acid into the diethyl ester, followed by a reduction with $LiAlD_4$ yields 1,1,2,2,5,5,6,6-octadeuterohexanediol. The reduction leads to the anticipated 100% deuterium exchange as verified by ^{1}H NMR. Bromination using a mixture of HBr and H_2SO_4 leads to the corresponding dibromo compound which was used in the alkylation of diethyl malonate. The previously presented procedures [13, 14]: reduction, ketal protection, coupling and finally deprotection, furnish the 2-[6-[4-[(4-cyanophenyl)azo]phenoxy]-1,1,2,2,5,5,6,6-octadeuterohexyl]-1,3-propanediol (**9**).

2.2. Instrumentation. Differential Scanning Calorimetry (DSC)

Calorimetric measurements of the monomers have been performed on a Perkin Elmer DSC 4 Differential Scanning Calorimeter equipped with a System 4 Thermal Analysis Microprocessor Controller and a Perkin Elmer 3600 Data Station. Heating and cooling cycles of mesogenic diols were carried out on 7 to 12 mg samples with a rate of 3°C/min covering a temperature range from 70°C to 170°C; in case of diphenyl esters the range was 20°C to 120°C.

Nuclear Magnetic Resonance (NMR) Spectroscopy

^{13}C, ^{1}H and ^{2}H NMR experiments were performed on a Bruker Avance DPX 250 NMR-spectrometer. Proton decoupled ^{13}C NMR spectra of the precursors were recorded at 62.9 MHz employing 3 to 4% (w/v) $CDCl_3$

solutions in 5-mm-i.d. tubes at 300 K. ^{13}C NMR spectra of the diol monomers were similarly obtained in $(CD_3)_2SO$. Accumulation of at least 20,000 scans, each consisting of a 9 μs 90° rf-pulse, followed by a 1.652-s pulse acquisition time with a subsequent relaxation delay of 1 s, was necessary to observe the multiplet structure of the appropriate ^{13}C signals due to the $^{13}C - {}^{2}H$ spin–spin coupling with maximum achievable intensity and resolution. The chemical shifts are referenced to the central resonance of $CDCl_3$ (76.90 ppm from tetramethylsilane (TMS)) or of $(CD_3)_2SO$ (37.60 ppm from TMS), respectively. ^{2}H NMR spectra were recorded at 38.4 MHz on the diphenyl ester solutions used for the ^{13}C NMR experiments after exchanging $CDCl_3$ with $CHCl_3$. In case of mesogenic diols the original $(CD_3)_2SO$ solutions were employed. 32 scans with a pulse width of 13 μs, an acquisition time of 1.367 s and a relaxation delay of 1 s were coadded. ^{1}H NMR data were obtained at 250.13 MHz from 1% (w/v) $CDCl_3$ or $(CD_3)_2SO$ solutions. 50 scans (11.5 μs 90° rf-pulse, 3.185 s acquisition time, 1 s relaxation delay) were accumulated. Chemical shifts for ^{1}H NMR are referenced to the resonance of (residual) $CHCl_3$ (7.26 ppm from TMS) or $(CH_3)_2SO$ (2.49 ppm from TMS). The resonance signal of residual $CDCl_3$ and $(CD_3)_2SO$ in the ^{2}H NMR spectra have correspondingly been defined as 7.24 and 2.49 ppm, respectively.

Fourier-Transform Infrared (FTIR) Spectroscopy

A Perkin-Elmer 1760X FTIR spectrometer equipped with a Perkin-Elmer IR Data Manager collecting and analysis system was employed to record IR spectra in the $4000 - 400\,cm^{-1}$ range; usually an average of 32 scans was accumulated with a resolution of $4\,cm^{-1}$. The crystalline samples were finely dispersed in a matrix of KBr from which a pellet has been prepared. The maximum absorbances ranges between 1 and 1.5.

UV-visible Absorption Spectroscopy

A Varian Cary 1E UV-Visible Spectrophotometer was employed to record UV-visible spectra of the diols as approx. 0.01 mg/mL tetrahydrofuran solutions.

Polarizing Optical Microscopy (POM)

The POM investigations were carried out using an Olympus BH-2 polarizing microscope equipped with a Mettler FP-82HT hot stage, controlled by a Mettler FP-90 unit.

3. RESULTS AND DISCUSSION

The structural elements of the desired liquid crystalline side-chain polyesters can be divided into the four different components indicated in Figure 1. The specific deuteration is achieved by separate labeling the building blocks which serve as precursors or monomers for the desired polyesters.

Deuterium labeling of the aliphatic polyester main-chain can partly be achieved by use of perdeuterated dicarboxylic acid precursors. With the previously adopted synthetic polyester strategy [14] in mind diphenyl perdeuterated tetradecanedioate (**2**) and adipate (**4**) were prepared. The melting points of **2** (80.9°C) and **4** (109.3°C) only deviate slightly from the previously established values of the corresponding non-deuterated analogues **3** (tetradecanedioate, 84.2°C) and **5** (adipate, 108.8°C) [25]. Thus, a noticeable difference (approx. 3°C [27]) is only experienced in the tetradecanedioate case where a great number of protons have been exchanged with deuterons.

The spectral implications of deuteration, on the other hand, are much more evident. Figure 2 shows the ^{1}HNMR spectrum of diphenyl perdeuterated tetradecanedioate (**2**).

Upon integration of the resonance signals in Figure 2, the degree of deuteration can be calculated to exceed 93%. Therefore, no detectable back

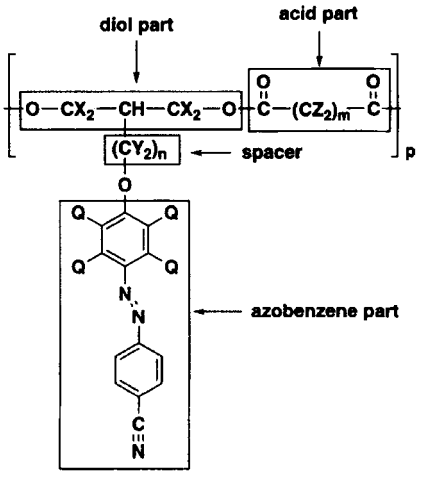

FIGURE 1 Structural building blocks of azobenzene side-chain polyesters.

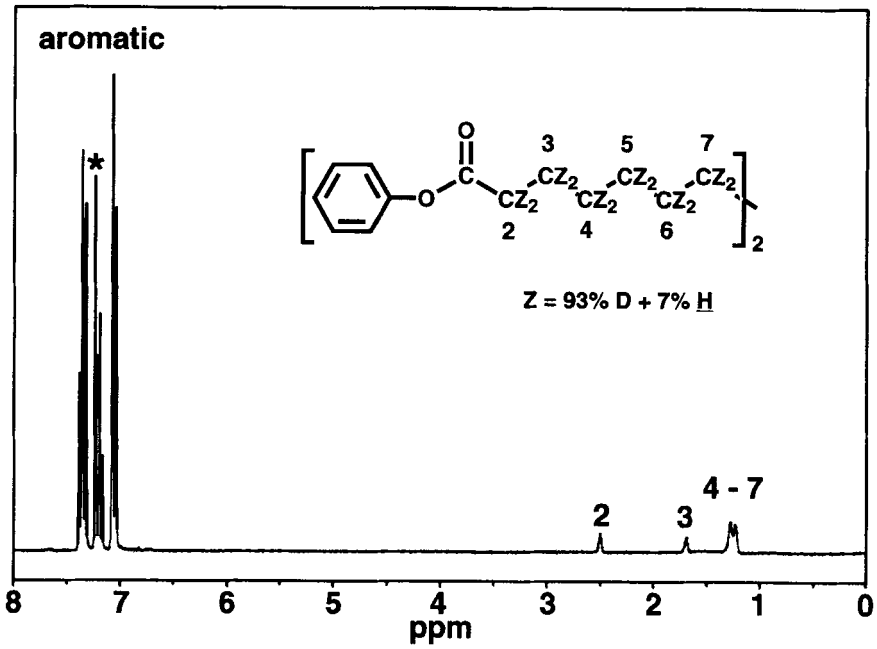

FIGURE 2 ^{1}H NMR spectrum of diphenyl perdeuterated tetradecanedioate (**2**) in $CDCl_3$ (* residual $CHCl_3$).

exchange is associated with the conversion of the acid into the diphenyl ester (**2**). Furthermore, the ^{1}H NMR spectrum shows that the incorporated deuterium is statistically distributed along the aliphatic chain. Obviously, determination of the deuterium content by ^{1}H NMR is an indirect analysis, the absence of protons is detected rather than the presence of deuterons. Hence, in order to illustrate the analysis of the deuterium incorporation, Figure 3 presents the ^{2}H NMR spectrum of the diphenyl perdeuterated tetradecanedioate (**2**). The three signals can be assigned to deuterium atoms in the α and β position (2 and 3) relative to the ester carbonyl groups and to the remaining aliphatic chain consisting of 8 CD_2 units (4–7); chemical shifts are listed in Table II which also contains the ^{1}H corresponding shifts. The integral values correspond to the 1 : 1:4 ratio of magnetically non-equivalent CD_2 groups and therefore confirm the uniform distribution of incorporated deuterium.

Figure 4 shows the corresponding ^{13}C NMR spectrum. Deuterium exchange is indicated by the vanishing of specific sharp ^{13}C signals in the resonance region of aliphatic carbons between 20 and 40 ppm. Due to

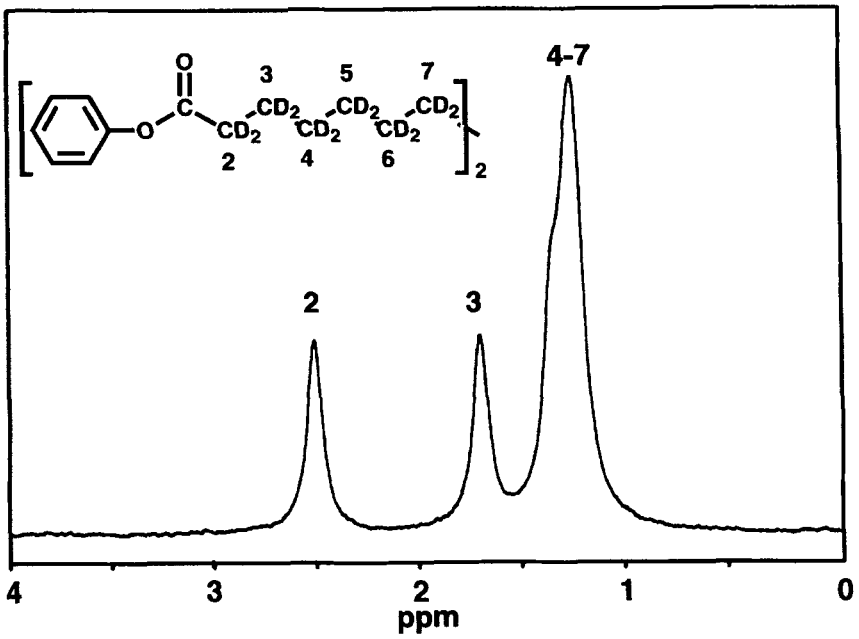

FIGURE 3 ^{2}H NMR spectrum of diphenyl perdeuterated tetradecanedioate (**2**) in $CHCl_3$.

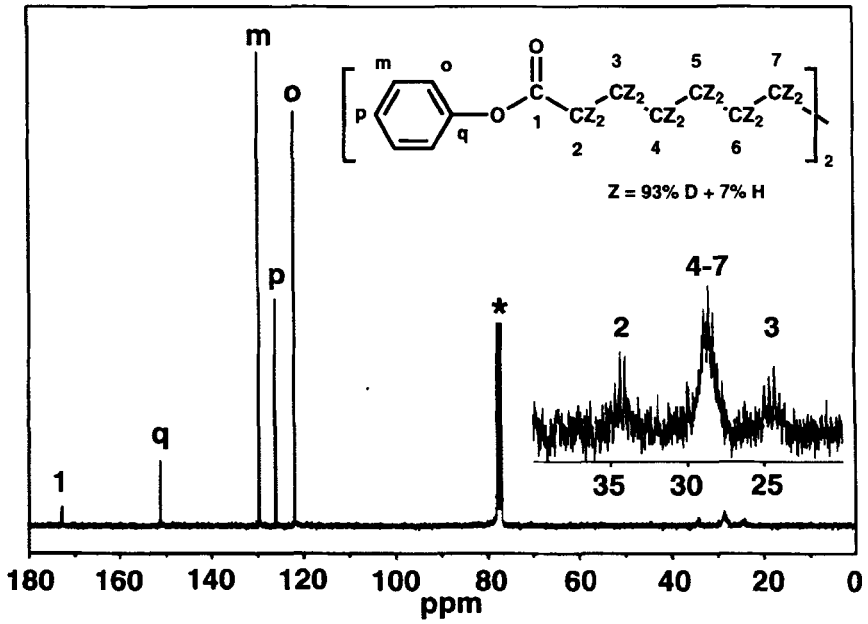

FIGURE 4 ^{13}C NMR spectrum of diphenyl perdeuterated tetradecanedioate (**2**) in $CDCl_3$ (*).

spin–spin coupling between adjacent ^{13}C and ^{2}H nuclei, a replacement of protons by deuterons results in a splitting of the corresponding ^{13}C NMR resonance into a multiplet structure which in the present case is difficult to resolve. The entire ^{13}C chemical shifts of perdeuterated (**2** and **4**) and corresponding non-deuterated [25] (**3** and **5**) diphenyl esters are collected in Table I. The ^{2}H NMR information on **2** and **4** is likewise summarized in Table II.

Figure 5 shows the FTIR spectra of the diphenyl tetradecanedioates, **2** and **3**. The spectra exhibit the absorption characteristics anticipated for this type of compounds. Different group vibrations, associated with the aliphatic methylene units, the phenoxy rings and the carboxyl groups, can be identified throughout the spectral region. The identified infrared vibrations [28] are listed in Table III which also contains similar information on the homologues diphenyl adipates **4** and **5**.

The behaviour of a molecular vibration can – to a first approximation – be described by a mechanical model. The vibrational frequency of a

TABLE I 62.9 MHz ^{13}C NMR chemical shifts of diphenyl esters (ppm in $CDCl_3$)

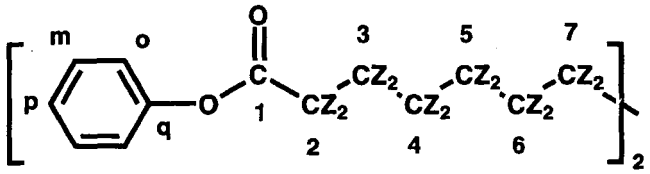

Ester	*Parent acid*	*Z*	1	2	3	4	5	6	7	*q*	*o*	*m*	*p*
2	tetradeca-nedioic	D	172.26	33.81	23.80	28.12	28.12	28.12	28.12	150.67	121.47	129.26	125.58
3	tetradeca-nedioic	H	172.14	34.25	24.79	28.94	29.08	29.30	29.37	150.67	121.44	129.23	125.56
4	adipic	D	171.68	33.02	23.06					150.49	121.40	129.28	125.67
5	adipic	H	171.63	33.85	24.17					150.59	121.44	129.30	125.70

TABLE II 38.4 MHz ^{2}H NMR chemical shifts of diphenyl esters (ppm in $CHCl_3$)

Ester	*Parent acid*	2[a]	3[a]	4–7[a]
2	tetradecanedioic	2.48 (2.54)[b]	1.68 (1.77)[b]	1.23 (1.35 + 1.29)[b]
4	adipic	2.59 (2.68)[c]	1.83 (1.89)[c]	

[a] Numbering refers to positions of deuterons in ester structures of Figure 3.
[b] Corresponding 250.13 MHz ^{1}H NMR chemical shifts of the non-deuterated analogue (**3**).
[c] Corresponding 250.13 MHz ^{1}H NMR chemical shifts of the non-deuterated analogue (**5**).

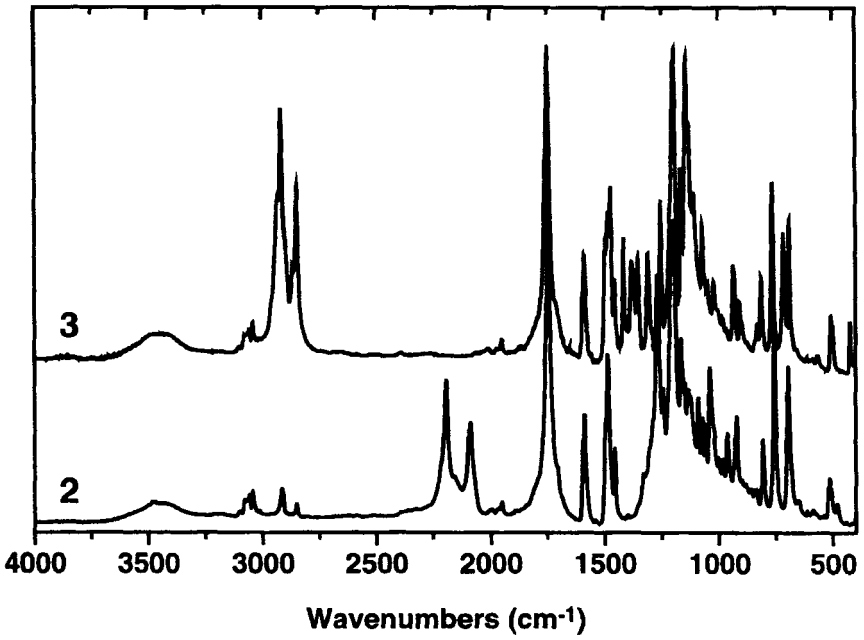

FIGURE 5 FTIR spectra of diphenyl tetradecanedioates; **2** with perdeuterated aliphatic chain, **3** non-deuterated.

TABLE III Band assignments and frequencies (cm^{-1}) of infrared absorptions of selectively deuterated and non-deuterated diphenyl adipate and tetradecanedioate

Band assignment	**2**	**3**	**4**	**5**
$\nu(CH)_{ar}$	3102–3042	3102–3042	3100–3043	3100–3043
$\nu_{as}(O{=}C{-}\mathbf{CH_2})$		2932		2957
$\nu_{as}(CH_2)$	2915[a]	2916		2942
$\nu_s(O{=}C{-}\mathbf{CH_2})$		2867		2918
$\nu_s(CH_2)$	2851[a]	2849		2873
$\nu_{as}(CD_2)$	2193[b]		2225[b]	
$\nu_s(CD_2)$	2090[b]		2116[b]	
$\nu(C{=}O)$	1746	1750	1753	1757
$\nu(C{=}C)_{ar}$	1590	1590	1592	1590
	1497 + 1487	1496 + 1484	1497 + 1485	1496 + 1483
$\delta(CH_2)$		1474		1462
$\delta(O{=}C{-}\mathbf{CH_2})$		1418		1414
$\omega(CH_2)$		1381–1355		1376
$\tau(CH_2)$		1312		...[c]
$\nu_{as}(C{-}C{-}O)$	1200	1197	1193	1195
$\delta(CD_2)$	1092		1082	
$\delta(O{=}C{-}\mathbf{CD_2})$	1060		1056	
$\omega(CD_2)$	1041		1057	
$\gamma(CH)_{ar}$	757	764	756	769
$\rho(CH_2)$		718		713
$\delta(C{=}C)_{ar}$	695	690	693	687

[a] Residual weak $\nu(CH_2)$ absorptions.
[b] Relatively broad and structured absorptions.
[c] Not identified.

diatomic oscillator, ν, depends on the force constant of the chemical bond, k, and the reduced mass, μ, of the attached atoms in the following way [29]:

$$\nu = \frac{1}{2\pi} \cdot \sqrt{\frac{k}{\mu}}$$

where $\mu = m_1 \cdot m_2/(m_1 + m_2)$. Replacing the proton in an oscillating (C—H) system by a deuteron increases the reduced mass and therefore, results in a shift of the related vibrational frequency towards lower wavenumbers. Accordingly, deuterium exchange in the aliphatic chain of **2** results in the disappearance of (CH_2) deformation (1470 – 1300 cm^{-1}) and stretching vibrations (3000 – 2800 cm^{-1}), as well as in band shift effects for various (C—C) skeletal modes (< 1100 cm^{-1}). As a consequence, absorptions due to equivalent (CD_2) stretching vibrations occur as two additional bands at 2193 and 2090 cm^{-1}, respectively. Due to the high response ability of aliphatic (CH_2) stretching vibrations to infrared radiation, even small deviations from a complete deuterium exchange (*ca.* 7%) can be detected in this particular spectral region of **2**. Identification and assignment of (CD_2) deformation vibrations (δ, ω, τ) can only be achieved by a systematic spectral analysis comparing different selectively deuterated as well as non-deuterated species.

The synthesis of the mesogenic 2-substituted-1,3-propanediols has been described briefly recently [13, 14] and is shortly reviewed in Figure 6.

The synthesis is based on the alkylation of diethyl malonate with dibromohexane followed by a mixed hydride reduction of the alkylation product yielding 2-(6-bromohexyl)-1,3-propanediol. Through ketal protection of the diol, using acetophenone, a 2-methyl-2-phenyl-5-(6-bromohexyl)-1,3-dioxane is obtained. This is coupled to a 4-[(4-cyanophenyl)azo]-phenol. Subsequent deprotection yeilds 2-[6-[4-[(4-cyanophenyl)azo]phenoxy]hexyl]-1,3-propanediol (**6**). In order to gain the necessary purity for the polycondensation process, the product has been recrystallized from ethanol and finally vacuum distilled.

Specific labeling of one of the aromatic cores, parts of the hexyl spacer and the propyl unit of the 2-substituted-1,3-propanediols has been accomplished using suitably deuterated reagents or appropriate preparative methods. Table IV illustrates the three different positions of deuterium labeling of the 2-substituted-1,3-propanediols. Labeling of the azobenzene moiety for instance will provide an analytical probe well suited for alternative instrumental investigations of the light induced isomerization process of the azobenzene chromophore. A 2-[6-[4-[(4-cyanophenyl)azo]-

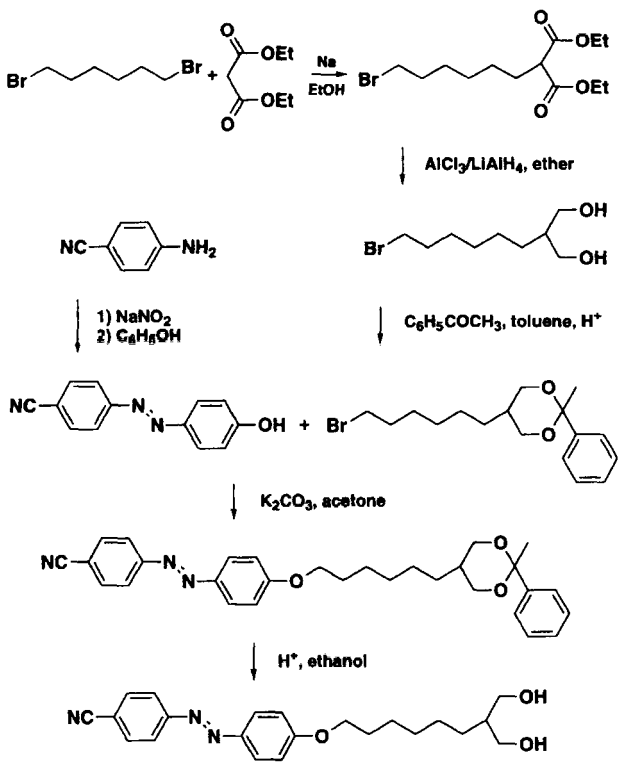

FIGURE 6 Synthetic scheme for preparation of 2-[6-[4-[(4-cyanophenyl)azo]phenoxy]hexyl]-1,3-propanediol (**6**).

TABLE IV Position of selective deuteration in 2-[6-[4-[(4-cyanophenyl)azo]phenoxy]hexyl]-1,3-propanediols

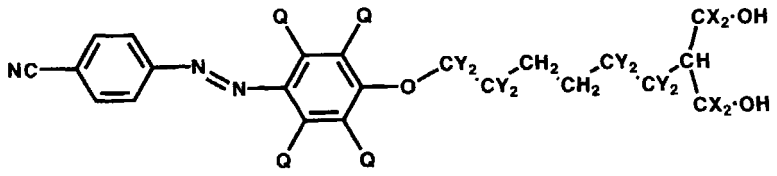

Diol	*Q*	*X*	*Y*
6	H	H	H
7	D	H	H
8	H	D	H
9	H	H	D

2,3,5,6-tetradeutero-phenoxy]hexyl]-1,3-propanediol (**7**) was synthesized by coupling the ketal protected diol with 4-[(4-cyanophenyl)azo]-2, 3,5,6-tetradeuterophenol which in turn was based on hexadeuterophenol. Employing $LiAlD_4$ in the reduction step, a 2-[6-[4-[(4-cyanophenyl)azo]-phenoxy]hexyl]-1,1,3,3-tetradeutero-1,3-propanediol (**8**) is obtained. This monomer has the potential of specifically label the diol part of the polyester main chain. Employed in combination with the diphenyl perdeuterated dicarboxylates the preparation of polyester main chains in which all methylene groups are deuterated will be possible. Furthermore, a deuterated handle directly on the flexible side-chain spacer is obtained through the partially deuterated aliphatic 1,1,2,2,5,5,6,6-octadeuterohexyl spacer. This was prepared starting from 2,2,5,5-tetradeuteroadipic acid (Fig. 7).

The resulting 1,6-dibromo-1,1,2,2,5,5,6,6-octadeuterohexane was employed in the initial alkylation of the malonate followed by the above sequence of reactions to furnish 2-[6-[4-[(4-cyanophenyl)azo]phenoxy]-1,1,2,2,5,5,6,6-octadeuterohexyl]-1,3-propanediol (**9**).

An absorption spectrum of **7** representative of the four azobenzene 1,3-propanediols is shown in Figure 8. The spectrum shows the intense $\pi-\pi^*$ band at 365 nm (ε 28,000 L mol^{-1} cm^{-1}) and a much weaker $n-\pi^*$ transition at 445 nm (ε 2,300 L mol^{-1} cm^{-1}). Similar values were determined for the homologues diols, **6**, **8** and **9**. These absorption patterns are characteristic of *trans* azobenzene containing compounds [30] although the position of both bands strongly depends on the nature of the substituents on the azobenzene

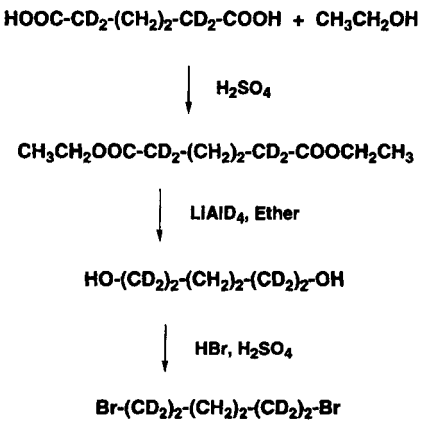

FIGURE 7 Synthetic scheme for preparation of 1,1,2,2,5,5,6,6-octadeutero-1,6-dibromo-hexane.

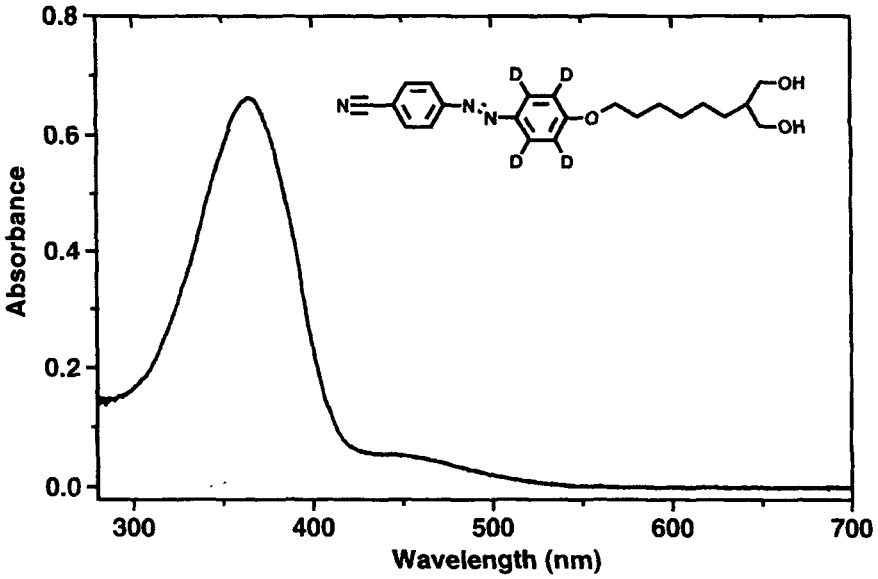

FIGURE 8 Visible absorption spectrum of 2-[6-[4-[(4-cyanophenyl)azo]-2,3,5,6-tetradeuterophenoxy]hexyl]-1,3-propanediol (7).

moiety. In contrast to the other spectroscopies to be discussed no deuterium isotope effect is observed on the visible absorption.

All the prepared diols have been thoroughly characterized by multinuclei NMR spectroscopy.

A ^{13}C NMR spectrum of **9** representative of all the diols is shown in Figure 9. Here it can be seen that all non-symmetrical carbons have ^{13}C resonances which due to the multitude of chemical functionality contained in these molecules are clearly separated and spread over a wide spectral range. The generally established spectral implications of functionality and additivity [31] in combination with findings for 4-hydroxyazobenzene [32, 33] have been employed in the assignments of the individual carbon resonances also listed in Table V.

The assignments of the aromatic carbons were further assisted by the intensity differences as observed in Figure 9. The hydrogen-bearing aromatic carbons in double presence form one group. This leaves a second group of basically differently substituted aromatic carbons all with relatively small intensities. Additionally, the assignments have also benefited by supplementary information [34] from an extensive range of similar azobenzene diols with other substituents. A partial confirmation of the reported

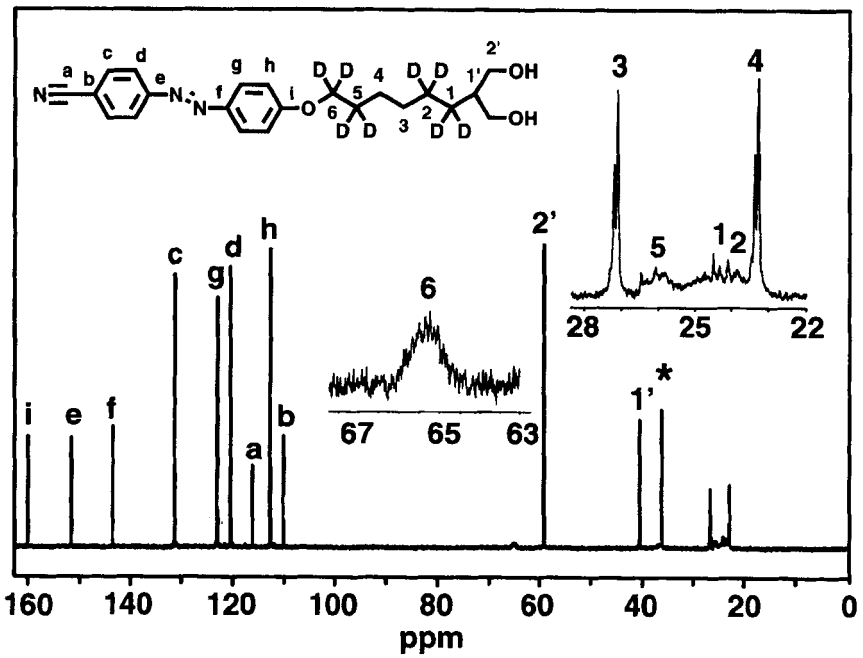

FIGURE 9 ^{13}C NMR spectrum of 2-[6-[4-[(4-cyanophenyl)azo]phenoxy]-1,1,2,2,5,5,6,6,-octadeuterohexyl]-1,3-propanediol (**9**) in $(CD_3)_2SO$ (*).

aromatic carbon assignments is obtained by the presence of deuterium in one of the aromatic cores in **7**. A closer inspection of Table V shows that the carbons (g and h) with directly attached deuterium are shielded approx. 0.4 ppm as compared to non-deuterated moieties in the isomeric diols **6**, **8** and **9**. However, also the neighbor carbons (f and i) without deuterium experience an approx. 0.1 ppm isotope effect. Primary (one-bond) and secondary (two-bond) deuterium isotope effects on aromatic ^{13}C nuclear shieldings on the order of 0.3 and 0.1 ppm, respectively, are normally observed [35], quite in line with the present observations. In the aliphatic region intensity differences due to the double presence of the hydroxyl groups distinguish and unequivocally identify the two oxymethylene carbon resonances (6 and 2′). This is actually confirmed by the isotope effects observable in diol **8**; here carbon 2′ is shielded approx. 0.8 ppm, but also the methine carbon (1′) experiences an approx. 0.3 ppm shielding as compared to carbons with the pure hydrogen environments in **6** and **7**. Generally, for straight-chain CD_2 groups an isotope effect of 0.36 ppm per D has been observed and the effects are largely additive whereas the effects over two

TABLE V 62.9 MHz ^{13}C NMR chemical shifts of 2-[6-[4-[(4-cyanophenyl)azo]phenoxy]hexyl]-1,3-propanediols (ppm in $(CD_3)_2SO$)

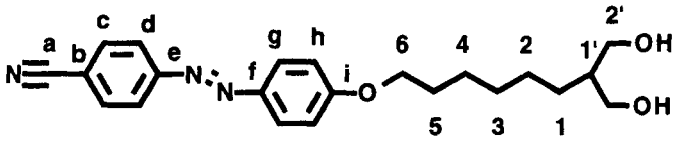

Diol	*a*	*b*	*c*	*d*	*e*	*f*	*g*	*h*	*i*	6	5	4	3	2	1	1′	2′
6	116.57	110.60	131.78	120.94	152.33	144.12	123.38	113.22	160.53	66.24	26.65	23.52	27.34	24.65	25.66	41.20	59.73
7	116.60	110.58	131.80	120.96	152.27	144.00	123.01	112.90	160.47	66.26	26.64	23.53	27.36	24.66	25.69	41.21	59.73
8	116.62	110.60	131.83	120.98	152.24	144.10	123.41	113.27	160.55	66.25	26.67	23.56	27.39	24.68	25.59	40.86	58.88
9	116.64	110.61	131.85	121.00	152.26	144.10	123.43	113.29	160.59	65.42	26.08	23.23	27.15	24.10	24.50	41.04	59.67

bonds usually are smaller than 0.1 ppm [35]. In diol **9** (shown in Fig. 9) the majority of the hexamethylenes are deuterium labeled. This leaves carbons 4 and 3 with no directly attached deuterium but influenced from the respective deuterium substituted neighbor carbons and accordingly shielded 0.2–0.3 ppm. The secondary effect although smaller can also be observed here on the methine carbon (1′). The primary isotope effect, on the other hand, can be observed at all the carbons 6, 5, 2 and 1 varying in the range 0.6 – 1.1 ppm. However, more precise values could possibly be obtained by selective deuteron decoupling thus suppressing the multiplicity of the carbon-deuteron resonances.

A ^{2}H NMR spectrum of diol **9** is shown in Figure 10. The ^{2}H chemical shifts of all the diols are collected in Table VI which additionally contains the corresponding proton information. ^{1}H NMR data of the diols have primarily served as a tool for a quantitative determination of the deuterium content and in the assignment of the corresponding ^{2}H NMR resonances assuming equivalent shift effects. In case of diol **7** the deuteration was calculated to 95% in the relevant positions, whereas the exchange by

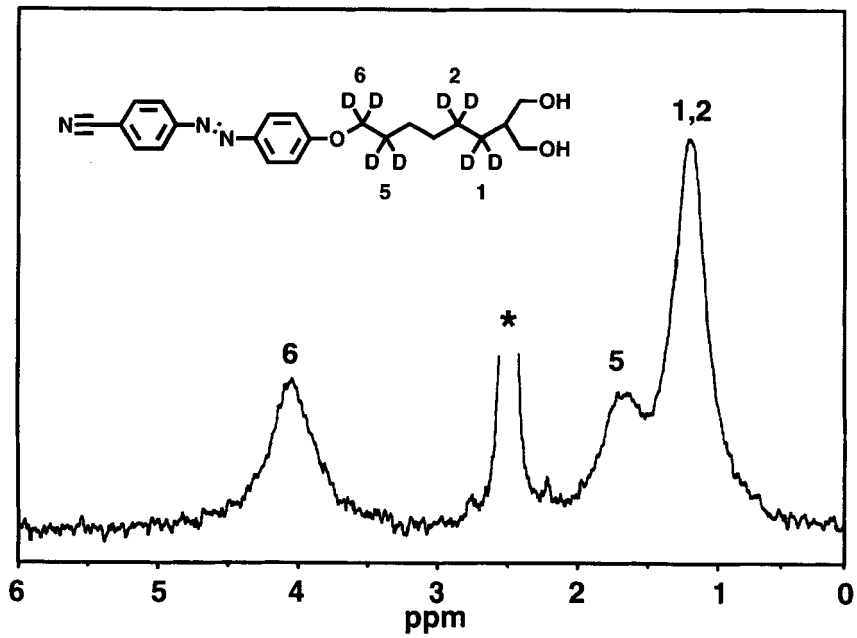

FIGURE 10 ^{2}H NMR spectrum of 2-[6-[4-[(4-cyanophenyl)phenoxy]-1,1,2,2,5,5,6,6-octadeuterohexyl]-1,3-propanediol (**9**) in $CHCl_3$ (* residual $(CD_3)_2SO$).

TABLE VI 38.4 MHz ^{2}H NMR chemical shifts of 2-[6-[4-[(4-cyanophenyl)azo]phenoxy] hexyl]-1,3-propanediols (ppm in $(CD_3)_2SO$)

Diol	*h*[a]	*g*[a]	6[a]	5[a]	2[a]	1[a]	2'[a]
7	7.19 (7.10)[b]	7.98 (7.89)[b]					
8							3.31 (3.36)[b]
9			4.04 (4.05)[b]	1.68 (1.70)[b]	1.19 (1.24)[b]	1.19 (1.24)[b]	

[a] Numbering refers to positions of deuterons in diol structure of Table V.
[b] Corresponding 250 MHz ^{1}H NMR chemical shifts of the non-deuterated analogue (**6**).

reduction leads to 100% deuteration in diol **8**. A detailed analysis of the diol proton spectra is not performed due to the presence of complex spin patterns in the aromatic region resulting in overlapping, poorly resolved resonance signals.

The four isomeric diols **6**–**9**, also have very similar FTIR spectra. Two representative spectra of finely dispersed **6** and **9** in a matrix of KBr are shown in Figure 11. The spectral features in both cases are governed by

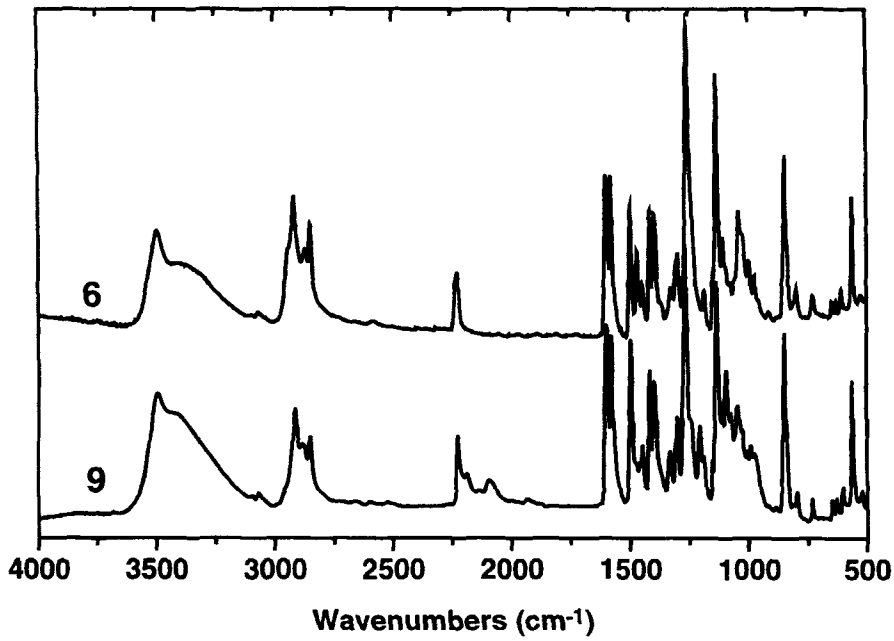

FIGURE 11 FTIR spectra of 2-[6-[4-[(4-cyanophenyl)azo]phenoxy]hexyl]-1,3-propanediol (**6**) and 2-[6-[4-[(4-cyanophenyl)azo]phenoxy]-1,1,2,2,5,5,6,6-octadeutero-hexyl]-1,3-propanediol (**9**).

characteristic group vibrations indicating the structural similarities, namely the broad ν(OH) band centered around 3444 cm^{-1}, the symmetric and asymmetric (CH_2) stretching vibrations in the 3000 to 2800 cm^{-1} range and particularly the $\nu(C\equiv N)$ band at 2227 cm^{-1}. In the fingerprint region, absorptions can be assigned to the aromatic azobenzene core (1603, 1582, 1500 and 849 cm^{-1}) and the aryl-alkyl ether vibration (1262 cm^{-1}). A detailed list of the identified infrared bands of all the diols are collected in Table VII.

The most obvious effect of selective deuterium exchange on the infrared spectrum of **9** is the appearance of two additional bands at 2185 and 2094 cm^{-1}, respectively. Since these spectral positions correspond satisfactorily with the expected frequency shift, estimated for the asymmetric and symmetric (CH_2) stretching vibrations as a consequence of deuterium exchange, these bands can therefore be assigned to the corresponding (CD_2) modes. However, the associated (CD_2) bending vibration appears at 1095 cm^{-1}. Specific deuterium labeling of methylene groups located at different molecular sites, effects also the complex absorption pattern in the

TABLE VII Band assignments and frequencies (cm^{-1}) of infrared absorptions of 2-[6-[4-[(4-cyanophenyl)azo]phenoxy]hexyl]-1,3-propanediols with deuteration in different positions

Band assignment	**6**	**7**	**8**	**9**
ν(OH)[a]	3497	3497	3497	3492
ν(OH)	3403	3403	3403	3426
$\nu(CH)_{ar}$	3070 + 3041	3055 + 3039	3069 + 3041	3068 + 3040
ν_{as} (—O—**CH_2**)[b]	2945	2946	2946	
$\nu_{as}(CH_2)$	2918	2918	2918	2912
ν_s (—O—**CH_2**)[b]	2872	2875	2873	
$\nu_s(CH_2)$	2851	2851	2851	2851
$\nu(CD)_{ar}$		2294 + 2281		
$\nu(C\equiv N)$	2227	2227	2227	2227
$\nu_{as}(CD_2)$			2189	2185
$\nu_s(CD_2)$			2089	2089
$\nu(C=C)_{ar}$	1603 + 1582	1576 + 1553	1603 + 1581	1602 + 1581
		1441	1499	1496
$\delta(CH_2)$	1471	–[c]	1471	–[c]
$\omega(CH_2)$	1329	–[c]	1330	1331
ν_{as} (Ar—O—R)	1262	1229	1262	1271
ν (Ar— N= N—Ar)[d]	1137	1136[e]	1137	1137
$\delta(CD_2)$			–[c]	1095
ν (C —O)	1044	1044	–[c]	1046
ν_s (Ar—O—R)	1025	989	1025	–[c]
$\gamma(CH)_{ar}$	849	848	848	849

[a] Relatively sharp and intense band, due to a dimeric or intramolecular associated structure.
[b] Aryl-alkyl ether.
[c] Not identified.
[d] Intense azobenzene related vibration, polarized in direction of the molecular long axis.
[e] Weak.

region of asymmetric and symmetric (CH_2) stretching vibrations (3000–2800 cm^{-1}). Aromatic (CD) stretching vibrations in the infrared spectrum of **7** can be observed as very weak absorption bands at 2294 and 2281 cm^{-1}, respectively (Tab. VII). Beside this primary isotope effect, directly observable on aromatic (C—D) absorptions, a secondary effect is reflected in the absorption spectrum of **7** causing frequency shifts and intensity variations of group vibrations associated with the aromatic azobenzene rings. Considerable changes are mainly induced in the fingerprint region and can be used to allocate infrared absorptions attributable to the azobenzene moiety. The entire shift of aromatic ring stretching modes rather than observing an equivalent splitting due to the presence of a labeled and a non-labeled ring counterpart, indicates a strong vibrational coupling between these modes throughout the conjugated azobenzene system.

Samples of the diols **6**–**9**, in the form of fine grains or powder on glass slides without cover slip, show invariably birefringent textures characteristic of crystalline compounds when observed in the dark field of the polarizing optical microscope. All the samples heated on the microscope hot stage at rates of 1–3°C/min melt rather sharply without apparent mesophase formation. However, on cooling the samples from their isotropic melt to lower temperature, the transition to solid crystal pertinent to the smallest and randomly distributed portions of the sample undergo the effect of supercooling, with subsequent formation of liquid crystalline state. On the contrary, the largest and thickest portions of the sample do not show apparent supercooling, and crystallize invariably. Anyway through careful POM observations of the diols it was possible to identify the schlieren and focal conic textures typical of nematic and smectic A phases, respectively, extended over the most part of the preparation area. Representative textures obtained upon cooling diol **9** from the melt are shown in Figure 12. The phase transformations as observed by POM and corresponding sequence of transition temperatures of all the diols **6**–**9**, are listed in Table VIII. For the smectic A to crystalline transition, only a temperature interval can be reported, due to the strong tendency of smectic mesophases to supercool. Furthermore, it is clearly seen from the data of Table VIII that deuteration does not affect the number and type of the phases identified through optical investigation of the diols during heating and cooling cycles.

The phase behaviour of the diols **6**–**9** was also investigated by differential scanning calorimetry (DSC). Figure 13 shows traces of the second heating and subsequent cooling cycle of diol **9**. The corresponding transition temperatures and enthalpies are additionally collected and compared with the relevant POM observations of all the diols, **6**–**9**, in Table VIII.

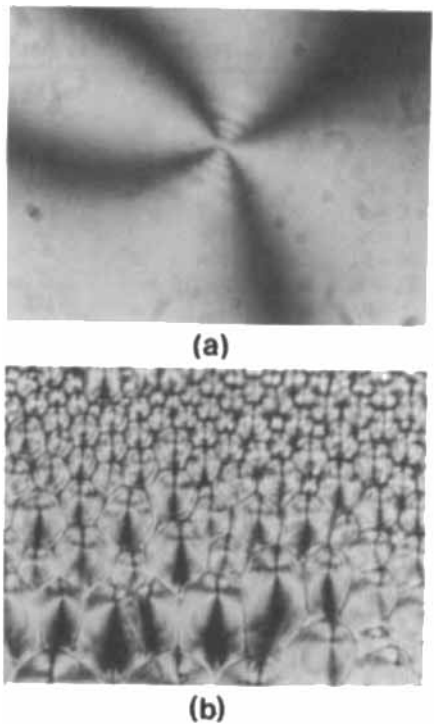

FIGURE 12 Photomicrographs showing optical textures obtained upon cooling diol **9** from the melt. (a) nematic schlieren texture at 135°C; (b) focal conic texture of smectic A at 131 °C. Crossed polarizers; magnification *x* 320.

This table clearly displays the essential features of the phase behaviour of all the diols, **6**–**9**. All the mesophases identified by POM have been obtained only by supercooling during the transition from the isotropic melt to the crystalline state. Therefore, these phases represent metastable states and diols **6**–**9** should be classified as monotropic liquid crystals. Furthermore, the monotropism has been confirmed by DSC measurements for diol **9**, as illustrated in Figure 12. On the other hand, for diols **6** and **7** the corresponding heating and cooling DSC traces only display single melting and crystallization peaks, without giving rise to substantial supercooling effect necessary for the mesophase formation. As regards the assignment of the relevant transition energies to the mesophase observed for the diols **8** and **9**, this was done on the basis of the comparison between the measured transition temperatures and the observed optical textures. The inclusion of the behaviour of the non-deuterated diol, **6**, in Table VIII allows for a direct

TABLE VIII Phase behaviour and transition temperatures of 2-[6-[4-[(4-cyanophenyl)azo]-phenoxy]hexyl]-1,3-propanediols with deuteration in different positions

Diol	*Transition*[a]	*Temperature (°C)*		ΔH^c
		by POM[b]	*by DSC*[b]	*(kJ/mol)*
6	K → I	152	153	46.8
	I → N	139		
	N → S_A	134		
	S_A → K	125–116		
	I → K		145	−46.8
7	K → I	151	157	47.4
	I → N	139		
	N → S_A	134		
	S_A → K	125–116		
	I → K		148	−46.5
8	K → I	152	153	41.1
	I → N	140	139	−1.0
	N → S_A	133		
	S_A → K	125–116		
	N → K		136	−36.6
9	K → I	151	151	40.3
	I → N	137	136	−1.3
	N → S_A	133	131	−0.3
	S_A → K	125–116	128	−35.9

[a] K: crystalline, I: isotropic melt, N: nematic, S_A: smectic A.
[b] Heating and cooling rates 3°C/min.
[c] Transition enthalpies as determined by DSC.

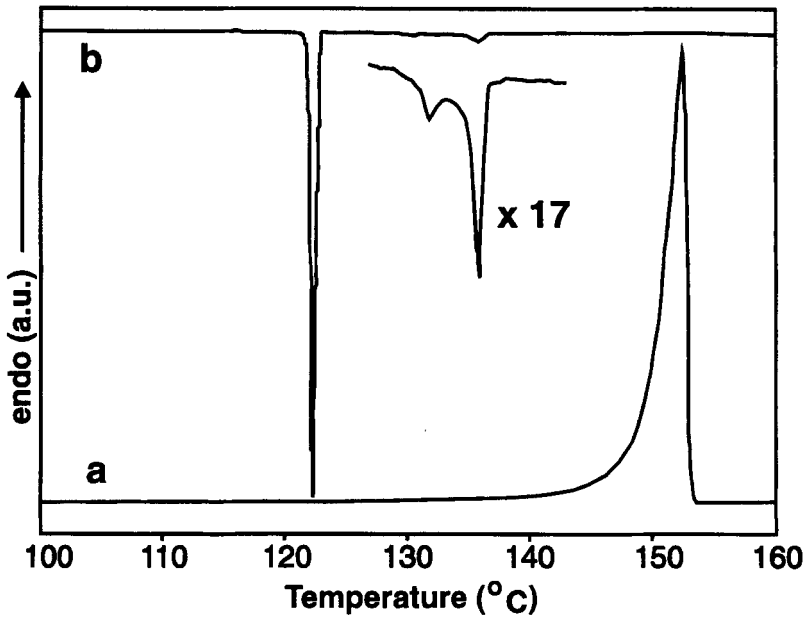

FIGURE 13 DSC traces of the second heating (a) and subsequent cooling (b) cycle of diol **9** (insert enlarged 17 *x*).

comparison which clearly reveals that deuteration only has a minor, almost negligible isotope effect on the mesomorphic phase behaviour of the partly deuterated liquid crystalline monomers, **7**–**9**.

4. CONCLUSIONS

The principles for strategic deuteration of selected precursors and diol monomers suitable for side-chain liquid crystalline polyester preparation have been outlined and exploited. Diphenyl perdeuterated adipate and tetradecanedioate; and three different, selectively labeled 2-[6-[4-[(4-cyanophenyl)azo]phenoxy]hexyl]-1,3-propanediols were prepared employing catalyzed deuterium exchange and reduction techniques at the appropriate synthetic steps. In this way it was possible to synthesize precursors and monomers carrying an isotope content between 90% and 100%. Furthermore, ^{13}C and ^{1}H NMR investigations reveal a statistical distribution of deuterium in case of extended perdeuterated aliphatic chains. The comparison between carbon-deuteron and carbon-hydrogen vibrations reveals a substantial frequency shift enabling an unequivocal spectral discrimination between hydrogen and deuteron methylene groups and accordingly the corresponding structural segments. All the selectively deuterated 2-[6-[4-[(4-cyanophenyl)azo]phenoxy]hexyl]-1,3-propanediols exhibit liquid crystalline phase behaviour comparable to the non-deuterated analogue. Thus, all the deuterated precursors and monomers have appreciable resonance and vibrational spectral isotope effects. On the other hand, only marginal differences were detected in the thermal properties between corresponding deuterated and non-deuterated isomers.

In addition to the synthesized polyester building blocks also a thorough and effective set of powerful, analytical tools has been exploited. A subsequent paper deals with the preparation and characterization of selectively deuterated liquid crystalline cyanoazobenzene side-chain polyesters.

Acknowledgements

C. K. and S. H. (Risø National Laboratory) gratefully acknowledge the financial support for this research from The Danish Polymer Centre supported by the Danish Materials Technology Development Programme (MUP 2). C. H., H. W. S. (University of Essen) and F. A. (CNR) extend their thank to the Brite/EuRam Programme under contract BRE2.CT93.0449.

References

[1] C. B. McArdle, Side Chain Liquid Crystal Polymers (Blackie and Son Ltd., Glasgow, U.K., 1989), Chap. 13, pp. 357–394, and cited literature.
[2] J. A. Chilton and M. T. Gossey, Special Polymers for Electronic and Optoelectronics (Chapman and Hall, London, U.K., 1995).
[3] H. Rau, Photochemistry and Photophysics (CRC Press, Inc., Boca Raton, Florida, 1990), Vol. II, Chap. 4, p. 119.
[4] W. M. Gibbons, P. J. Shannon, S.-T. Sun and B. J. Swetlin, *Nature*, **351**, 49 (1991).
[5] A. G. Chen and D. J. Brady, *Opt. Lett.*, **17**, 441 (1992).
[6] A. Natansohn, P. Rochon, J. Gosselin and S. Xie, *Macromolecules*, **25**, 2268 (1992).
[7] S. Xie, A. Natansohn and P. Rochon, *Chem. Mat.*, **5**, 403 (1993).
[8] M. Eich, J. H. Wendorff, B. Reck and H. Ringsdorf, *Makromol. Chem. Rapid Commun.*, **8**, 59 (1987).
[9] K. Anderle, R. Birenheide, M. Eich and J. H. Wendorff, *Makromol. Chem. Rapid Commun.*, **10**, 477 (1989).
[10] U. Wiesner, M. Antonietti, C. Boeffel and H. W. Spiess, *Makromol. Chem.*, **191**, 2133 (1990).
[11] J. Stumpe, L. Muller and D. Kreysig, *Makromol. Chem. Rapid Commun.*, **12**, 81 (1991).
[12] H. J. Haitjema, G. L. von Morgen, Y. Y. Tan and G. Challa, *Macromolecules*, **27**, 6201 (1994).
[13] S. Hvilsted, F. Andruzzi and P. S. Ramanujam, *Opt. Lett.*, **17**, 1234 (1992).
[14] S. Hvilsted, F. Andruzzi, C. Kulinna, H. W. Siesler and P. S. Ramanujam, *Macromolecules*, **28**, 2172 (1995).
[15] P. S. Ramanujam, C. Holme, S. Hvilsted, M. Pedersen, F. Andruzzi, M. Paci, E. L. Tassi, P. L. Magagnini, U. Hoffman, I. Zebger and H. W. Siesler, *Polym. Adv. Techn.*, **7**, 768 (1996).
[16] N. C. R. Holme, P. S. Ramanujam and S. Hvilsted, *Opt. Lett.*, **21**, 902 (1996).
[17] C. Kulinna, I. Zebger, S. Hvilsted, P. S. Ramanujam and H. W. Siesler, *Macromol. Symp.*, **83**, 169 (1994).
[18] P. S. Ramanujam, S. Hvilsted, I. Zebger and H. W. Siesler, *Macromol. Rapid Commun.*, **16**, 455 (1995).
[19] N. C. R. Holme, P. S. Ramanujam and S. Hvilsted, *Appl. Opt.*, **35**, 4622 (1996).
[20] P. S. Ramanujam, N. C. R. Holme and S. Hvilsted, *Appl. Phys. Lett.*, **68**, 1239 (1996).
[21] H. W. Spiess, *J. Chem. Phys.*, **72**, 6755 (1980).
[22] H. W. Spiess, *Pure and Appl. Chem.*, **57**, 1617 (1985).
[23] H. Zimmermann, *Liq. Cryst.*, **4**, 591 (1989).
[24] M. W. Neubert, *Mol. Cryst. Liq. Cryst.*, **129**, 327 (1985).
[25] S. Hvilsted, F. Andruzzi, P. Cerrai and M. Tricoli, *Polymer*, **32**, 127 (1991).
[26] H. G. Atkinson, J. J. Csakvary, G. T. Herbert and R. S. Stuart, *J. Am. Chem. Soc.*, **90**, 498 (1968).
[27] The data are not directly comparable since the previously employed [25] heating rate was 5°C/min. However, the effect of the different heating rates are expected to be negligible.
[28] D. O. Hummel and F. Scholl, Atlas der Polymer- und Kunststoffanalyse (Carl Hanser Verlag, München, 1988), Vol. 2, Part b/I Text, p. 401.
[29] D. I. Bower and W. F. Maddams, The Vibrational Spectroscopy of Polymers (Cambridge University Press, Cambridge, UK, 1989), p. 135.
[30] H. Rau and E. Lüddecke, *J. Am. Chem. Soc.*, **104**, 1616 (1982).
[31] W. W. Simons, The Sadtler Guide to Carbon-13 NMR Spectra (Sadtler Heyden, Philadelphia, 1983).
[32] E. Lippmaa, T. Pehk, T. Saluvere and M. Mägi, *Org. Magn. Reson.*, **5**, 441 (1973).
[33] A. Lycka, D. Snobl, V. Machacek and M. Vacera, *Org. Magn. Reson.*, **15**, 390 (1981).
[34] M. Pedersen, New Azobenzene Side-Chain Polyesters for Optical Information Storage, *Ph.D. Thesis*, Technical University of Denmark (1997).
[35] P. A. Hansen, *Annu. Rep. NMR Spectrosc.*, **15**, 105 (1983).